Biophysical Journal
Article

Biophysical Society

Novel elasticity measurements reveal *C. elegans* cuticle stiffens with age and in a long-lived mutant

Mohammad Rahimi,[1,2] Salman Sohrabi,[1,2] and Coleen T. Murphy[1,*]
[1]Department of Molecular Biology & Lewis Sigler Institute for Integrative Genomics, Princeton University, Princeton, New Jersey

ABSTRACT Changes in biomechanical properties have profound impacts on human health. *C. elegans* might serve as a model for studying the molecular genetics of mammalian tissue decline. Previously, we found that collagens are required for insulin signaling mutants' long lifespan and that overexpression of specific collagens extends wild-type lifespan. However, whether these effects on lifespan are due to mechanical changes during aging has not yet been established. Here, we have developed two novel methods to study the cuticle: we measure mechanical properties of live animals using osmotic shock, and we directly perform the tensile test on isolated cuticles using microfluidic technology. Using these tools, we find that the cuticle, not the muscle, is responsible for changes in the "stretchiness" of *C. elegans*, and that cuticle stiffness is highly nonlinear and anisotropic. We also found that collagen mutations alter the integrity of the cuticle by significantly changing the elasticity. In addition, aging stiffens the cuticle under mechanical loads beyond the cuticle's healthy stretched state. Measurements of elasticity showed that long-lived *daf-2* mutants were considerably better at preventing progressive mechanical changes with age. These tests of *C. elegans* biophysical properties suggest that the cuticle is responsible for their resilience.

SIGNIFICANCE Aging is associated with changes in the mechanical properties of affected tissues, but the cause-and-effect aspect of these changes in aging has not yet been well established. *C. elegans* is a premier model organism to study age-related decline and longevity regulation, but its changes in mechanical properties with age and in long-lived mutants has not yet been explored. We have developed novel techniques to measure mechanical properties of *C. elegans* at the whole body and isolated cuticle scales, providing tools to study molecular pathways underlying changes in biophysical properties.

INTRODUCTION

The study of cell and tissue mechanics is crucial in understanding physiological and pathological processes and how they change with age. Mechanical forces play a major role in stem cell differentiation (1), cell migration (2), and cellular polarization (3). Moreover, most pathological conditions, such as orthopedic disorders, atherosclerosis (4), cancer (5), and neurodegenerative disorders (6), are associated with significant changes in the mechanical characteristics of cells. Aging, in particular, is associated with mechanical changes in tissues that may reduce overall life quality or accelerate aging (7,8). For instance, skin loses its elasticity, bones become brittle, and muscles lose mass. Stiffening of the vasculature with age is associated with cardiovascular disease, as well.

C. elegans is a premier model organism for studying age-related changes because of its high genetic tractability, optically transparent body, relatively simple cellular structure, and short lifespan. Like higher-order organisms, *C. elegans*' epithelial cells are essential for development and regulation of nutrients and ions coming from the outside environment. Hypodermal cells are the main component of the epithelial system and secrete the cuticle, which wraps around the whole body and forms an extremely flexible and resilient extracellular matrix. The nematode's cuticle is mainly composed of cross-linked collagens and additional insoluble proteins that are synthesized in hypodermal cells (9). Collagen provides strength, elasticity, and structural stability to fibrous tissues. Mutations in individual collagen genes result in defects in worm morphology (e.g., Dumpy and Blister mutants) and can cause embryonic and larval death (10). We previously discovered that the expression of many cuticle collagens that decrease with age remain high in long-lived *daf*-2 insulin signaling mutants and are required for their longevity (11). Moreover, the

Submitted October 6, 2021, and accepted for publication January 18, 2022.
[2]These authors contributed equally
*Correspondence: ctmurphy@princeton.edu
Editor: Guy Genin.
https://doi.org/10.1016/j.bpj.2022.01.013
© 2022 Biophysical Society.

overexpression of some of these collagen genes also extends the lifespan of wild-type animals (11). However, the mechanism by which these collagens alter the worm's lifespan is not clear.

To dissect molecular mechanisms of changes in worms' mechanical properties, we need a robust technique to measure the cuticle's stiffness. Various techniques have been developed to probe the mechanical properties of cells and tissues, including piezos (12), force probes (13), micropipette aspiration (14), optical tweezers (15), atomic force microscopy (AFM) (16), magnetic twisting cytometry (17), and microelectromechanical systems-based force clamp (18). Among them, a pressurized microfluidic chip (19) and AFM (20) have been used to probe *C. elegans* cuticle mechanics. Using volumetric compression measurements by applying hydrostatic pressure, it was suggested that the bulk mechanical properties of whole worms are independent of the cuticle, and that collagen mutants targeting the cuticle do not impact the bulk modulus (19). In contrast, a recent AFM study of *C. elegans* stiffness and topography suggested that there is a gradual loss in cuticle stiffness with age, and dietary restriction regimes directly influence the biomechanical properties of animals (20). However, AFM measurements are highly localized and can have considerably different elastic moduli (20), and may result in irreproducibility depending on the probe and contact mechanics model used. Thus, a more reliable technique for measuring the mechanical properties of worms may provide a better understanding of the role of the cuticle stiffness changes during *C. elegans* aging.

Here, we developed osmotic shock and tensile test techniques to measure stress-strain relationship and the elasticity of the cuticle at the whole body and isolated cuticle scales, and upon disruption by collagen mutation. We then investigated how mechanical strength correlates with age and in longevity mutants. Our results suggest that the cuticle's elasticity is highly nonlinear and anisotropic. Also, the elasticity of the *C. elegans* cuticle changes considerably with age, and this change is robustly delayed in the long-lived *daf-2* insulin receptor mutant.

MATERIALS AND METHODS

C. elegans strains and maintenance

C. elegans strains were grown at 20°C on nematode growth medium plates or high growth medium plates seeded with OP50 *Escherichia coli*. RNAi clones, including *col-120*, were obtained from the Ahringer RNAi library. The empty vector *L4440* RNAi clone was used as control. The following strains were used in this study: wild-type worms of the N2 Bristol strain, *daf-2(e1370)*, and *dpy-13(e184)*.

Osmotic shock

Worms were immobilized by 100 μM sodium azide in M9 buffer. Then they were deposited in high osmolarity solution by adjusting the concentration of sodium chloride. At 2 and 1 OSM solutions, the cuticle becomes completely flaccid, which indicates that the internal pressure is zero. Upon estimation of α and M_0 using volume shrinkage data points at these high osmolarities, a direct relationship between the osmolarity of the environment and the mechanical pressure on the cuticle as a function of volume can be determined. Then, animals were gradually and quasi-statically transferred from hyperosmotic medium to a hypoosmotic buffer. Body shape measurements after each transfer to solutions with various osmolarities were then used to calculate data points for internal pressure and cuticle strain. There should be a 20-min pause in each step to ensure that water exchange with the outside environment through the semipermeable cuticle is complete. Measurements can be done at high throughput by gradually adding deionized water to osmotic solutions in 96-well plate.

Our mathematical model can reliably calculate the cuticle's elastic moduli at large stretching loads during hypoosmotic shock for all mutants. The only limitation is the calculation of stiffness at smaller stretching loads for osmotic resistance mutants during hyperosmotic shock. The osmotic resistance phenotype interferes with our calculations of stiffness during hyperosmotic shock, as enhanced activation of glycerol synthesis counterbalances the high external osmotic pressure (21,22). It should be noted that the calculations of elastic moduli at smaller stretching loads for other mutants are not affected.

Cuticle isolation

The cuticle isolation protocol described by Cox et al. (23) was used. In brief, worms were collected and washed in M9 buffer three times and the supernatant was discarded. The *C. elegans* pellet was resuspend in 5 mL sonication buffer (10 mM Tris-HCl [pH 7.4], 1 mM EDTA) and then incubated on ice for 10 min. A total of 30 μL 0.1 M phenyl-methanesulfonyl fluoride was added to the solution, which was then sonicated several times for 20-s bursts with 20-s breaks on ice in between. Cuticles were washed several times with sonication buffer by centrifugation at 1500 rpm for 1 min and the supernatant was discarded. The solution was resuspended in 1 mL of ST buffer (1% SDS, 0.125 M Tris-HCl [pH 6.8]) and the tube was heated for 2 min at 100°C. Finally, cuticles were washed three times with 0.5% Triton-X in sterile ddH_2O by centrifuging at 3000 rpm for 1 min.

Microfluidic chip

The instructions for molding master fabrication, PDMS device fabrication, and measurement of closing pressures were adopted from Fordyce et al. (24) and McDonald and Whitesides (25). Three molds for the top, middle, and bottom parts of the stretch chip were fabricated using SU-8 2075 (MicroChem, Newton, MA) and spin coated at 2000 rpm for 30 s. PDMS (Sylgard 184, Dow Corning, Midland, MI, USA) mixed at 10:1 ratio was poured on these SU-8 molds. The mold for the middle layer was spin coated at 4000 rpm for 30 s to create a thin layer for the clamping section. To fabricate the membrane substrate, PDMS was poured on a blank substrate and spin coated at 4000 rpm for 5 min. All layers were half cured at 65°C for 40 min. The top and middle layers were aligned and cured at 65°C for 24 h. Thin PDMS membrane was also bonded to the bottom layer to be cured at 65°C for 24 h. Upon plasma treating the bottom section and bonding it to the glass slide, inlets and outlets were created using a 0.75-mm biopsy punch.

Statistics

For all comparisons between two groups, an unpaired Student's *t*-test was performed. For comparisons between multiple groups, one-way ANOVA was performed with post-hoc testing. GraphPad Prism was used for all statistical analyses.

RESULTS

Shrinking and swelling during osmotic shock

The cuticle is under hydrostatic pressure from internal tissues (19). The cuticle's anisotropic mechanical properties and the worm's internal pressure determine its shape in homeostasis (Fig. 1 *a*). The worm's cuticle is semipermeable to water and, upon transferring to the hypoosmotic solution, the worm swells until it explodes (Video S1). We can also reduce the internal pressure by applying a hyperosmotic

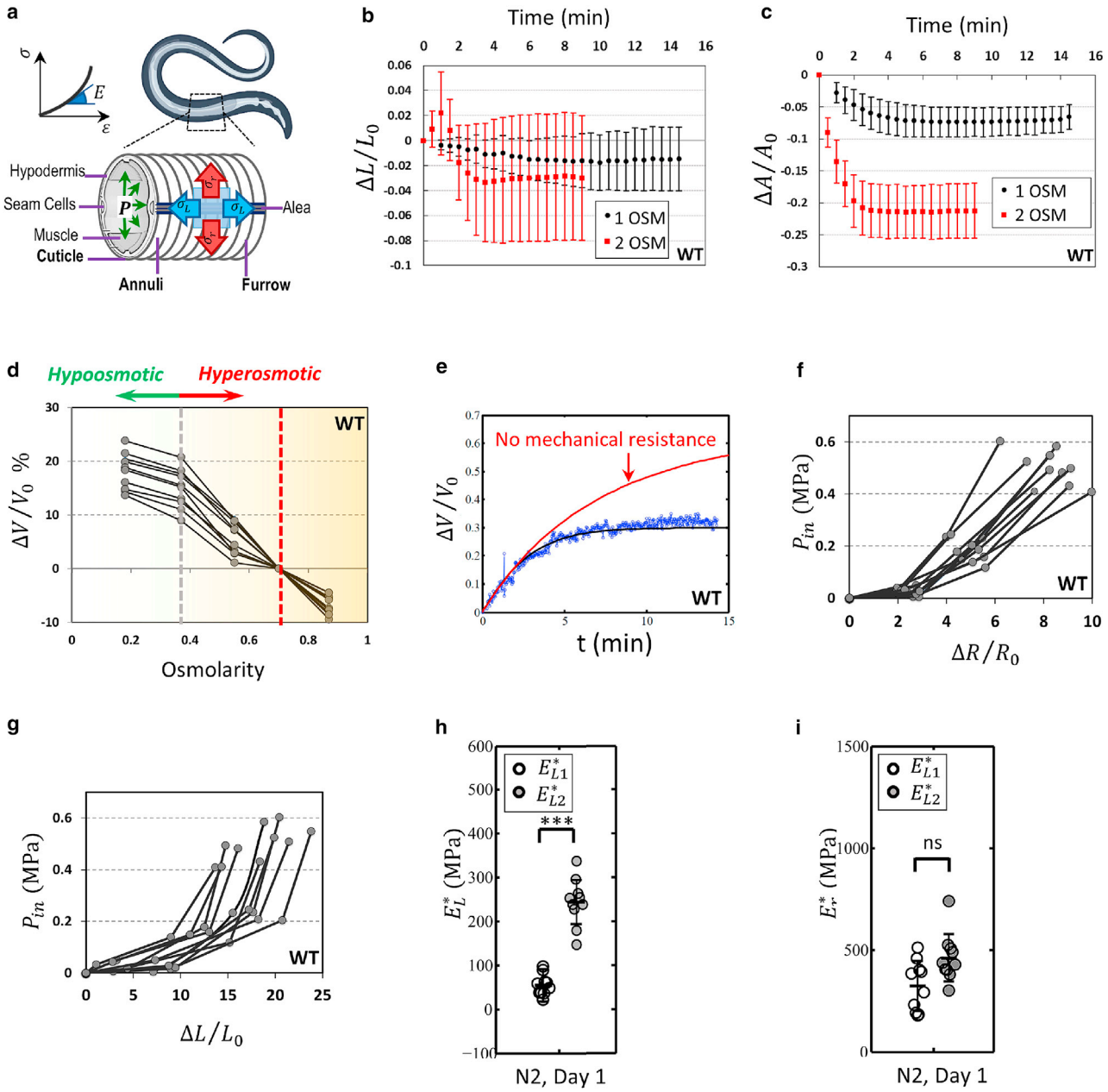

FIGURE 1 Anisotropic and nonlinear elasticity of *C. elegans*. (*a*) Internal pressure stretches *C. elegans*' cuticular structures (annuli, furrow, and alae). (*b* and *c*) Time course measurement of worms' length and projected area after transfer to high osmolarity solutions. Higher osmolarity solutions generate more overall shrinkage and it may take up to 20 min for water exchange to reach the steady state. $n = 10$ per condition. (*d*) Wild-type animals were transferred from hyperosmotic medium to hypoosmotic medium quasi-statically. V_0 is the volume of the flaccid worms. $n = 10$ per condition. (*e*) Time course measurement of volume upon transferring worms to lower osmolarity solution (0.55 to 0.25 OSM). Applying a mathematical model to these data points, we can estimate the mechanical force resisting swelling. V_0 is the initial volume of the animal before the osmotic shock. (*f* and *g*) Using our mathematical model and body shape change data, the internal pressure can be calculated. $n = 10$ per condition. Elastic moduli in radial (*h*) and longitudinal (*i*) directions for wild-type worms under small and large stretching loads. Wild-type animals have no osmotic resistance phenotype. $n = 10$ per condition; two biological replicates. Two-tailed *t*-tests. $^{***}p < 0.001$. Plots show 25th percentile, median, and 75th percentile. To see this figure in color, go online.

shock as the water exits and the body shrinks in an anisotropic manner (Video S2). A time course analysis of the changes in body shape was used to estimate the cuticle's stiffness based on these changes in shape.

The internal and external osmolarities reach equilibrium by exchanging water with the outside environment through its semipermeable cuticle. Volume exchange can be described as

$$\frac{d(\varepsilon_v)}{dt} = \frac{C_{\text{perm}}}{RT}\,[\Delta P_{osm} - \Delta P_{in}], \tag{1}$$

where R is the Boltzmann constant, T is temperature, C_{perm} is the permeability, ΔP_{osm} is osmotic pressure, and P_{in} is internal pressure. Osmotic pressure can also be rewritten as

$$\Delta P_{osm}(\varepsilon_v) = \text{RT}\left(\text{M}_{\text{out}} - \frac{\text{M}_0}{1 + \frac{1}{\alpha}\varepsilon_v}\right), \tag{2}$$

where M_0 is internal osmolarity, M_{out} is the osmolarity of the environment, and α is the water fraction of the worm's volume. $\text{M}_{\text{out}} = 0.345$ OSM is the healthy concentration for the worm's environment either in fluid or in agarose gel (26). Since the cuticle becomes wrinkled and flaccid at high osmolarities, the internal pressure of worms at 1 and 2 OSM solutions are assumed to be zero. We can record the projected area and length of worms to quantify body shape changes as animals are transferred to these high osmolarity solutions (Fig. 1, *b* and *c*). From there, normalized volume changes can be calculated using $\varepsilon_v = \Delta V/V_0 = (\Delta A/A_0) + (\Delta R/R_0)$ to estimate $\alpha = 0.65$ and $\text{M}_0 \cong 0.7$ OSM using Eq. 2. We then measured volume changes of animals with respect to their flaccid state at different osmolarities upon gradually transferring them from hyperosmotic medium to hypoosmotic buffer (Fig. 1 *d*). In our mathematical model, if there is no mechanical resistance (Eq. 1), the animal would exchange water until it reaches solution osmolality (Fig. 1 *e*). The difference between this prediction and our real-time volume change measurement demonstrates how much mechanical load is imposed on the cuticle in the form of internal pressure (Fig. 1, *f* and *g*). Various physiological features may contribute to the rate at which water and solutes transport across cuticle and lumen, permeability (C_{perm}). This transient state of body shape change enables quantifying C_{perm} (Eq. 1). Here, we have used the final equilibrium state to calculate mechanical pressure (Fig. 1, *b* and *c*), which avoids complications involving rates of solute transport.

Anisotropic nonlinear behavior of the cuticle

Our calculations of internal pressure demonstrated that it only slightly changes as M_{out} is increased to 0.55 OSM (Fig. 1, *f* and *g*). The additional increase in internal pressure resulted in nonlinear responses in length and radial changes under small and large stretching loads. The cuticle is always under this small stretching load when maintained on growth medium with healthy osmolarity. The larger stretching load happens during hypoosmotic shock, where the cuticle is stretched beyond its normal stretched state.

Incorporating local thickness into our derivations is complicated considering that aging changes the cuticle's morphology in a nonuniform and locally irregular fashion (27). In addition, cuticle thickness may vary between individual worms and across different mutants. To develop a universal standard approach to further examine the macroscale mechanics of the cuticle independent of microscale changes, we simplified the cuticle as a thin cylinder with 0.5 μm thickness to be the load-bearing component for internal pressure (Fig. S1 *a*). We can then plot stress-strain curves and accordingly calculate the elasticity of the cuticle, E^*, at different stretching loads (Fig. S1,*b* and *c*). Upon measurement of the local thickness (t), elastic moduli and stress at a specific location of worm's body can then be calculated using $\text{E} = \alpha\text{E}^*$, and $\sigma = \alpha\sigma^*$, where $\alpha = 0.5\ \mu\text{m}/t$.

We found that the cuticle is generally stiffer in the radial direction compared with the longitudinal direction, consistent with the presence of most structural collagen fibers, which are oriented in the azimuthal direction (Fig. 1, *h* and *i*). Moreover, due to a regular pattern of annular furrows on the cuticle in the longitudinal direction, the cuticle behavior is highly nonlinear under small and large stretching loads (Fig. 1 *h*). By contrast, the radial elasticity was not significantly different between these stretching loads (Fig. 1 *i*).

To properly distinguish between hypoosmotic and hyperosmotic measurements, the cuticle's response to hypoosmotic shock is discussed in terms of stiffness quantifiable by elastic moduli (E^*_{L2} and E^*_{r2}) (Figs. 2 and 3). In contrast, cuticle response to hyperosmotic shock is discussed in the term of resistance and compared using body shape changes ($\Delta L/L_0$ and $\Delta R/R_0$).

Collagen mutations alter integrity of the cuticle

Collagens are required for maintaining cuticle structure and barrier function in *C. elegans*. To investigate how collagen contributes to the elasticity and strength of cuticle, we have tested collagen mutants. Mutations in cuticle collagen genes with homozygous reduced or loss-of-function alleles, including *dpy-13(e184)*, result in a phenotype described as Dumpy (Dpy) and have narrower annuli than those of the wild-type worms (10). Together with two other closely related collagen genes, they constitute one of three distinct collagen subfamilies (28,29).

To reliably calculate stiffness during hyperosmotic shock using our mathematical model, tested mutants should not demonstrate osmotic resistance phenotype through activation of glycerol synthesis (21). *dpy-13* is reported to have

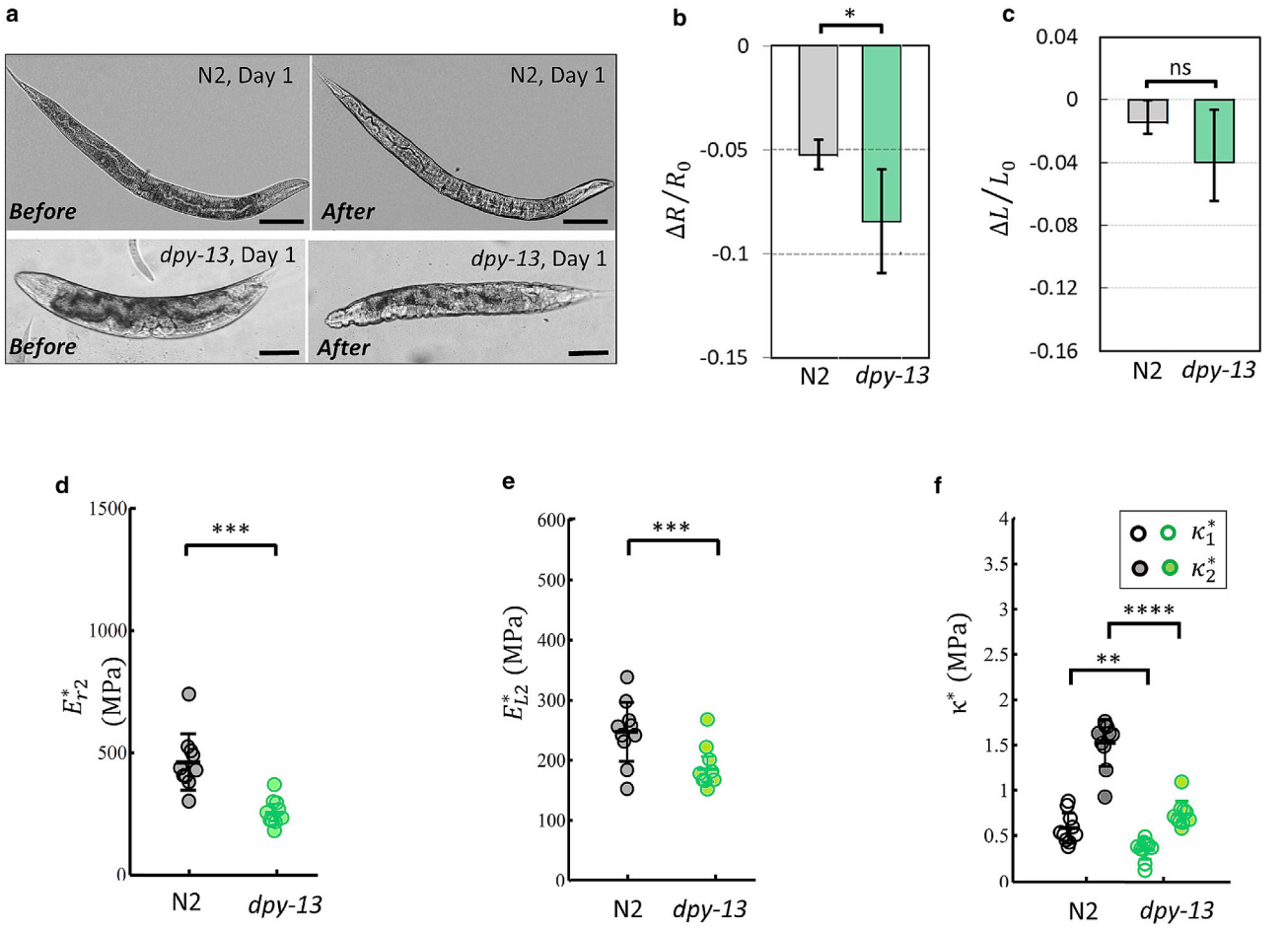

FIGURE 2 Collagen mutants have a softer cuticle. (*a*) Young wild-type and *dpy-13* worms' immediate response to hyperosmotic shock (0.35 to 1 OSM). The appearance of wrinkles in the young collagen gene mutant indicates a lower cuticular resistance. Scale bars, 100 μm. (*b* and *c*) Worms were transferred to 1 OSM solution and imaged after 20 min. Length and area changes of wild-type and *dpy-13* worms at day 1 were calculated; N2/day 1: $n = 12$, *dpy-13*/day 1: $n = 16$. (*d* and *e*) Elastic moduli in radial and longitudinal directions for young wild-type and collagen mutants. N2/day 1: $n = 10$, *dpy-13*/day 1: $n = 10$. (*f*) Bulk moduli of wild-type and collagen mutants under small and large stretching loads. The cuticle defective mutant is significantly softer than wild-type. N2/day 1: $n = 10$, *dpy-13*/day 1: $n = 10$; two biological replicates. Two-tailed *t*-tests. $^*p < 0.05$, $^{**}p < 0.01$, $^{***}p < 0.001$, $^{****}p < 0.0001$. Plots show 25th percentile, median, and 75th percentile. To see this figure in color, go online.

wild-type stress response with no osmotic resistance phenotype, suggesting that it would be amenable to a high osmolarity test (21,30). As *dpy-13* is predicted to be a structural constituent of the cuticle, disruption in cuticle development and collagen- and cuticulin-based cuticle molting cycle may lead to a softer cuticle (28,29,31); thus *dpy-13* mutants are optimal as a proof-of-principle test for new approaches to measure cuticle stiffness.

Upon transferring young adult animals from M9 buffer to high osmolarity solution, we found that the cuticles of young *dpy-13(e184)* mutants immediately became wrinkled compared with wild-type cuticles (Fig. 2 *a*). The larger radial shrinkage (Fig. 2 *b*) and significantly more elastic bulk modulus, κ_1^* (Fig. 2 *f*) of young *dpy-13* mutants indicated a lower hyperosmotic resistance compared with wild-type animals (Fig. 2). Similarly, under hypoosmotic swelling, *dpy-13* mutants also showed significantly lower radial and longitudinal stiffnesses compared with the wild-type (Fig. 2, *d* and *e*). These findings indicated that disruption in collagen function in cuticle development leads to a softer cuticle (Fig. 2 *f*), which correlates with the mutant's phenotypic defects.

Osmotic shock analysis of aged cuticles

Aging has a significant effect on the anisotropic mechanical properties of the cuticle (Fig. 3 *a*). We observed that aged (day 10) wild-type worms shrink considerably in the longitudinal direction in response to hyperosmotic shock (Fig. 3 *c*). Similarly, bulk moduli under small stretching loads also indicated softening of cuticles with age (Fig. 3 *f*). By contrast, our measurements of high stretching load with hypoosmotic swelling showed that the cuticle becomes significantly stiffer in both directions with age (Fig. 3, *d–f*).

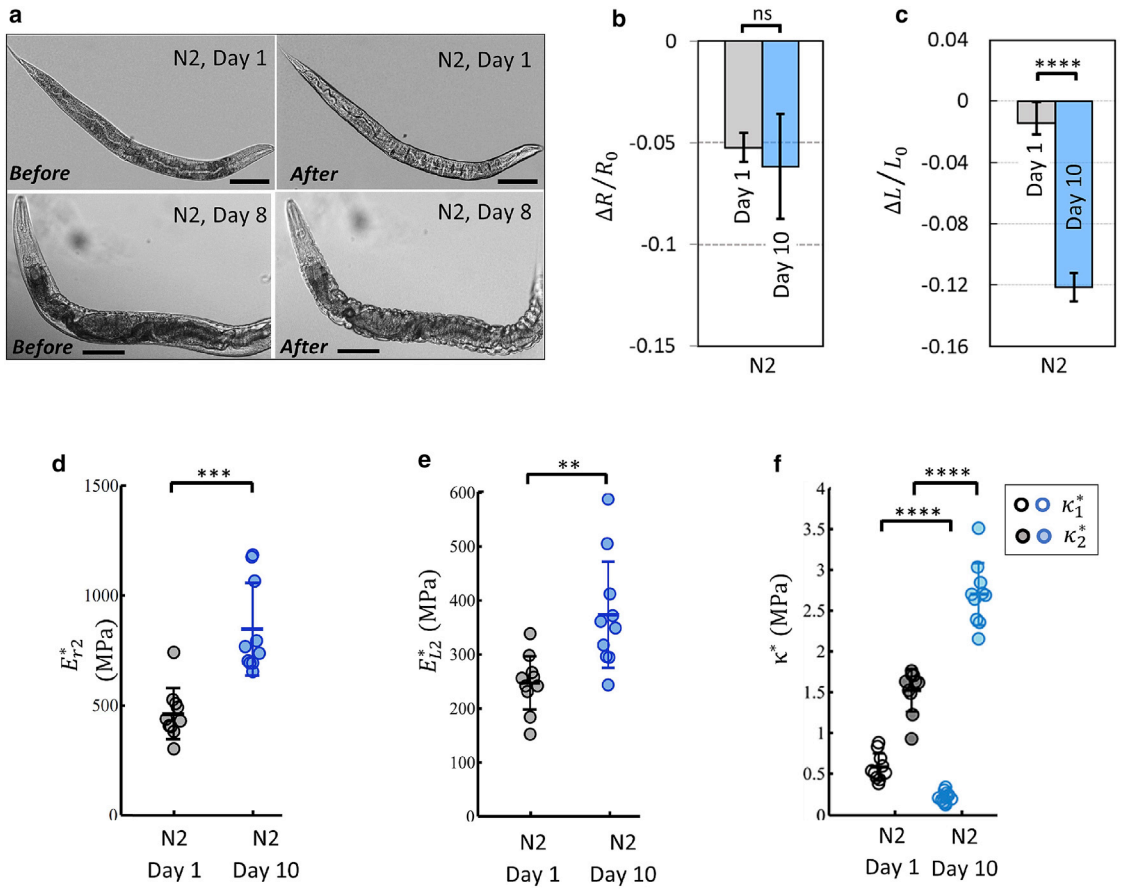

FIGURE 3 Aging alters the stiffness of the *C. elegans* cuticle. (*a*) Young and aged wild-type worms' immediate response to hyperosmotic shock (0.35 to 1 OSM). Scale bars 100 μm. (*b* and *c*) Worms were transferred to 1 OSM solution and imaged after 20 min. Length and area changes of wild-type worms at day 1 and day 10 were calculated; N2/day 1: $n = 12$, N2/day 10: $n = 8$. (*d* and *e*) Elastic moduli in radial and longitudinal directions for young and aged wild-type worms; N2/day 1: $n = 10$, N2/day 10: $n = 10$. (*f*) Bulk moduli of young and aged wild-type worms. The cuticle softens at small stretching loads and stiffens at larger stretching loads. N2/day 1: $n = 10$, N2/day 10: $n = 10$; two biological replicates. Two-tailed *t*-tests. $*p < 0.05$, $**p < 0.01$, $***p < 0.001$, $****p < 0.0001$. Plots show 25th percentile, median, and 75th percentile. To see this figure in color, go online.

Tensile test of isolated cuticles

Measurements of whole worms or intact worm bodies suggest that changes in the cuticle are responsible for the worm's stiffness, but do not rule out contributions from muscles or other tissues. Thus, we needed to directly measure the stiffness of the worm's cuticle to confirm that the osmotic shock technique measures changes in the cuticle. To do so, we first isolated intact cuticles from the worms (23). We built a three-layer microfluidic chip to stretch isolated cuticles, and measured the cuticle's membrane deflection h as a function of the applied pressure (Fig. 4, *a* and *b*). The push-up valve was first pressurized to measure the deflection of the membrane without the cuticle before initiating the tensile test (Fig. 4 *c*). Then, the isolated cuticle, free of cellular and membranous material, was adhered to a thin PDMS membrane and push-down valves were pressurized to clamp the cuticle (Fig. S1 *d*). The drop in membrane deflection compared with the deflection without the specimen represents the cuticle's resistance against stretching (Fig. 4 *c*).

Tensile test measurements of young and aged cuticles

Membrane deflections corresponding to chip pressure can be mathematically translated into strain and stress data points in the longitudinal direction. Therefore, osmotic shock measurements can be compared with the results from the direct tensile test of the isolated cuticle by calculating normalized length change using $\Delta L/L_0 = (\theta.R - a)/a$, where $R = (h^2 + a^2)/2h$, and $\sin(\theta) = a/R$ (Fig. S1 *e*). We found that stress-strain curves of isolated cuticles corroborate the results from our osmotic shock technique (Fig. 4 *d*). The slope of the stress-strain curve corresponds to the longitudinal elastic moduli, which decrease with age at small stretching loads. In contrast, the cuticle stiffens with age at larger stretching loads (Fig. 3 *e*).

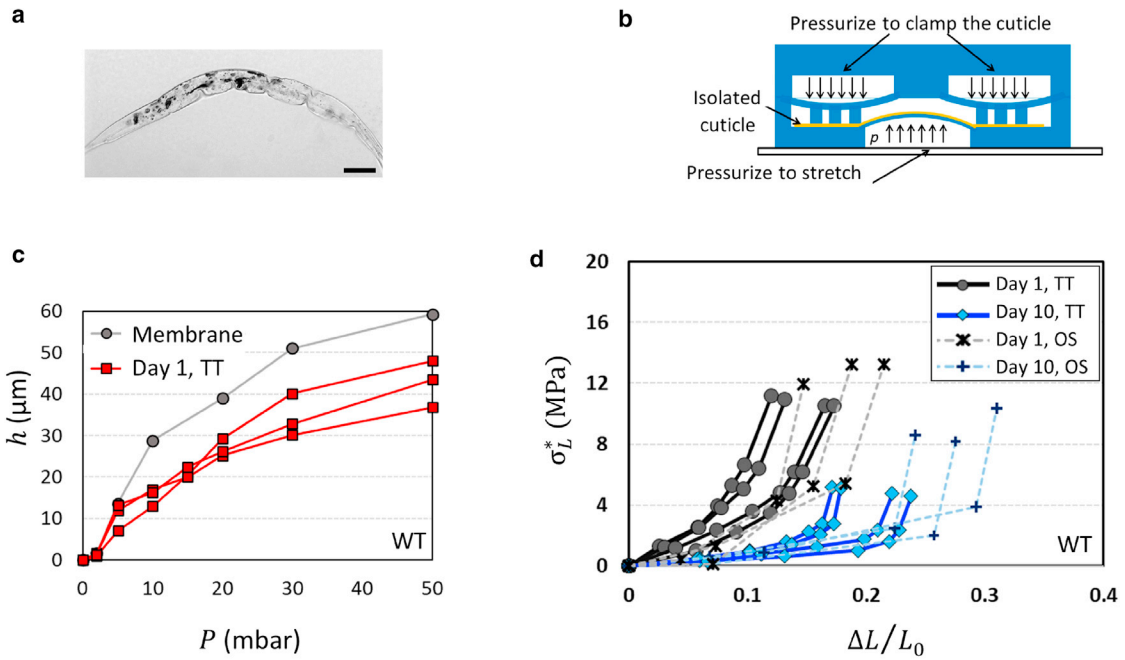

FIGURE 4 Tensile test of the cuticle using a microfluidic device. (*a*) The isolated cuticle is free of cellular and membranous material. Scale bar, 100 μm. (*b*) Side view of a three-layer chip to apply stretching force on an isolated cuticle. (*c*) The PDMS membrane was deflated using a pressure pump with and without the cuticle. The membrane deflection h was recorded as a function of the applied pressure P. N2/day 1: $n = 3$. (*d*) Agreement of stress-strain curves acquired using the tensile test (TT) with osmotic shock (OS) measurements. Aged (day 10) wild-type worms have higher stiffness than day 1 worms. N2/day 1/TT: $n = 4$, N2/day 10/TT: $n = 4$, N2/day 1/OS: $n = 3$, N2/day 10/OS: $n = 3$; two biological replicates. To see this figure in color, go online.

Osmotic shock analysis of long-lived *daf-2* mutants

We next tested long-lived *daf-2* insulin receptor mutants to determine whether their longevity is correlated with the mechanical characteristics of the cuticle. *daf-2* mutants increase lifespan through their regulation of a suite of genes that affect proteostasis, innate immunity, stress responses, fat stores, and metabolism, among other processes, including collagen expression (32–36). We observed that aged longevity mutants were considerably better at maintaining resistance under hyperosmotic shock at youthful levels (Fig. 5, *a–c*). Similarly, stiffness changes with age under swelling in both directions were robustly slowed in *daf-2*, while the wild-type cuticle becomes considerably stiffer (less elastic) with age (Fig. 5, *d* and *e*).

We previously showed that reduction of collagen gene expression during adulthood reduced *daf-2* lifespan, and that the overexpression of collagens extends wild-type lifespan (11). Among collagen genes required for *daf-2*'s long lifespan, *col-120*'s sequence is unique. Although adulthood RNA interference knockdown of *col-120* reduces *daf-2* lifespan, it did not affect affect body size and did not induce unfolded protein, heat shock stress, or oxidative stress responses (11). Therefore, *col-120* was chosen to test whether the reduction of collagens that affects *daf-2* lifespan does so by altering the mechanics of the epithelial system. Adulthood *col-120* knockdown in the *daf-2* mutant increased *daf-2*'s shrinkage to wild-type levels in aged (day 10) worms (Fig. 5 *f*), suggesting that loss of *col-120* reduces mechanical resistance of the *daf-2* cuticle. Thus, collagens are critical for the extended maintenance of elasticity in *daf-2* mutants.

DISCUSSION

Changes in mechanical properties with age can have profound impacts on health. For example, human arteries, which are scaffolded by elastin and collagen, progressively increase in stiffness more than twofold between the ages of 25 and 75 years (37), and this increased stiffness is associated with the development of cardiovascular disease. Aging causes collagen matrix to unravel, total collagen content to increase, cross-linking to occur, and collagen fiber distribution to disorganize, all of which lead to dysfunction, including arterial stiffening (38,39).

C. elegans is well suited for the study of age-related changes in tissue mechanics (11). However, few methods existed for studying cuticle mechanics. Here, we have introduced two novel, complementary techniques that allowed us to measure the mechanical properties of the cuticle. In our osmotic shock approach, quantifying the body shape change and calculating the worm's internal pressure allows us to use a mathematical model to estimate the anisotropic mechanical properties of the cuticle.

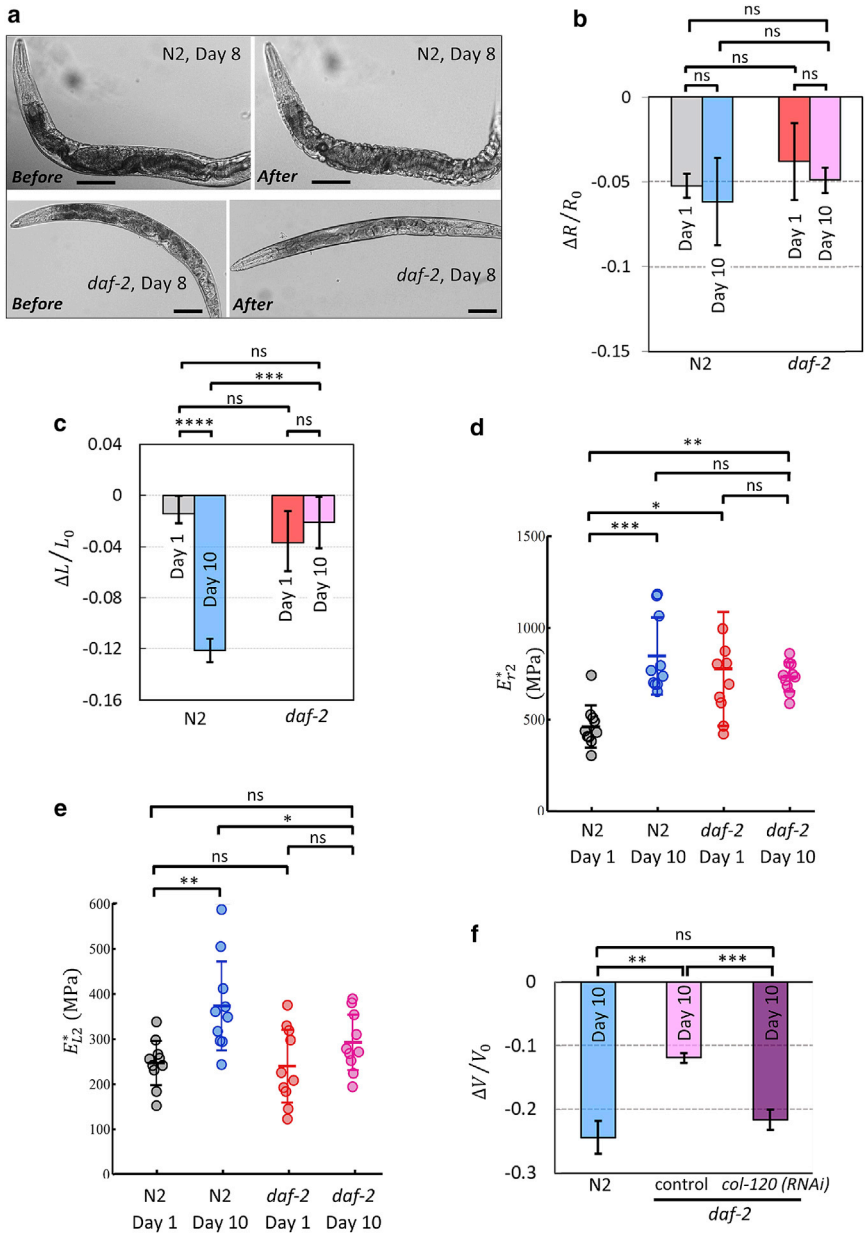

FIGURE 5 Stiffness changes with age are slowed in the *daf-2* longevity mutant. (*a*) Aged wild-type and *daf-2* worms' immediate response to hyperosmotic shock (0.35 to 1 OSM). Absence of wrinkles in the aged long-lived mutant signals better cuticle resistance. Scale bars, 100 μm. (*b* and *c*) Worms were transferred to 1 OSM solution and imaged after 20 min. Length and area changes of wild-type and *daf-2* worms at day 1 and day 10 were calculated. Decreasing resistance with age is slowed in *daf-2* mutant; N2/day 1: $n = 12$, N2/day 10: $n = 8$, *daf-2*/day 1: $n = 12$, *daf-2*/day 10: $n = 8$. (*d* and *e*) Elastic moduli in radial and longitudinal directions for young and aged wild-type and long-lived mutants. Increasing stiffness of cuticle with age is slowed down in *daf-2* mutant. N2/day 1: $n = 10$, N2/day 10: $n = 10$, *daf-2*/day 1: $n = 10$, *daf-2*/day 10: $n = 10$. (*f*) Adulthood collagen gene knockdown reduced *daf-2* ability to resist volumetric shrinkage upon transferring to 1 OSM solution. $n = 8$ for N2 and *daf-2;(control)*. $n = 14$ for *daf-2;(col-120 RNAi)*. Two biological replicates. One-way ANOVA with Dunnett's post-hoc. $*p < 0.05$, $**p < 0.01$, $***p < 0.001$, $****p < 0.0001$. Plots show 25th percentile, median, and 75th percentile. To see this figure in color, go online.

To confirm our results from osmotic shock, which is an indirect but high-throughput approach, we used microfluidic technology to stretch an isolated cuticle to measure stiffness in the longitudinal direction. Body size changes in the osmotic shock technique reproducibly produce a robust stress-strain curve by simplifying whole worms as an elastic thin cylinder, while the tensile test measures elasticity directly at considerably lower throughput (Video S3).

Previous measurements of cuticular local stiffness using a piezoelectric transducer indicated a high elastic modulus in the 380 MPa range (12). Another similar local stiffness study utilizing the buckling of nanowires reported an elastic modulus of 457 MPa on the lateral alae, and 257 MPa in the region immediately around the lateral alae (40). Our measurements of wild-type animals averaged at $E^*_{L2} \cong 250Mpa$ and $E^*_{r2} \cong 450Mpa$, which is in close agreement with these studies.

It was suggested that the bulk mechanical properties of whole, paraformaldehyde-fixed worms are independent of the cuticle (19). However, the excessive muscular stiffness induced by high paralytic concentrations or by fixation might have obscured these measurements, as we found that the cuticle rather than the muscle is the main component determining the stiffness of the worm. We also showed that, despite its relative thinness (roughly 2% of the diameter of the worm), the cuticle is responsible for whole-worm changes in "stretchiness" with age.

An AFM study of *C. elegans* stiffness and topography suggested that worms undergo a marked loss of stiffness and increased cuticle senescence during aging (20). However, our results suggest that the cuticle's behavior is highly nonlinear; while the cuticle softens at small stretching loads similar to AFM measurements, it stiffens at large stretching loads. These findings were confirmed using both osmotic shock and direct tensile tests. It is possible that the spherical probe in the AFM setup is only able to measure cuticle behavior with highly localized small indentation forces and cannot deliver a broader understanding of the anisotropic nonlinear mechanical properties of the whole worm or whole cuticle (20). These AFM measurements also showed that reduction of the IGF-1 signaling pathway preserved stiffness with age (20). Similarly, we also found that long-lived *daf-2* mutant worms were better at preventing progressive softening and stiffening with age under small and large stretching loads, respectively. Therefore, we believe that the approaches we describe here have provided a more comprehensive understanding of cuticle mechanics. We also tested a *Dumpy* mutant to investigate how defects in microstructure affect the mechanics of whole tissue and found the cuticle of *dpy-13* worms is significantly softer than wild-type cuticles. In addition, knocking down the extracellular structural genes that preserve the lifespan of longevity mutants altered the physical properties of the *C. elegans* exoskeleton and reduced the resistance of *daf-2* animals in response to osmotic shock.

Detailed mechanical studies of *C. elegans* will enable the characterization of a largely unexplored phenotype that has important consequences for human aging. Specifically, cuticle stiffness can be used as a biomarker for healthspan. Based on their specific attributes, these assays can be used to assess changes in body frailty of worms in vivo to probe the role of specific collagens in the regulation of longevity, pathogenesis, and osmotic stress regulation. Our results suggest that cuticle components help animals retain their "youthful" mechanical properties, particularly elasticity, with age. This elasticity may not only be a result of maintained youthfulness, but may also contribute to longevity. Overall, this work will provide the platform to integrate molecular genetics with biophysical measurements, providing a more complete understanding of the frailty of worms as they age.

SUPPORTING MATERIAL

Supporting material can be found online at https://doi.org/10.1016/j.bpj.2022.01.013.

AUTHOR CONTRIBUTIONS

M.R. and C.T.M. designed the experiments. M.R. performed the experiments. M.R., S.S., and C.T.M. analyzed the data. S.S. and C.T.M wrote the manuscript.

ACKNOWLEDGMENTS

We thank the *C. elegans* Genetics Center for strains (P40 OD010440) and the Murphy lab for discussion. This work was supported by the Glenn Foundation for Medical Research award to C.T.M. and a DP1 Pioneer (NIH) award to C.T.M. C.T.M. is the Director of the Glenn Center for Aging Research at Princeton and an HHMI-Simons Faculty Scholar.

REFERENCES

1. Datta, N., Q. P. Pham, …, A. G. Mikos. 2006. In vitro generated extracellular matrix and fluid shear stress synergistically enhance 3D osteoblastic differentiation. *Proc. Natl. Acad. Sci. U S A.* 103:2488–2493.
2. Wang, H. Q., L. X. Huang, …, Z. L. Jiang. 2006. Shear stress protects against endothelial regulation of vascular smooth muscle cell migration in a coculture system. *Endothelium.* 13:171–180.
3. Katsumi, A., A. W. Orr, …, M. A. Schwartz. 2004. Integrins in mechanotransduction. *J. Biol. Chem.* 279:12001–12004.
4. Slager, C. J., J. J. Wentzel, …, P. W. Serruys. 2005. The role of shear stress in the generation of rupture-prone vulnerable plaques. *Nat. Clin. Pract. Cardiovasc. Med.* 2:401–407.
5. Suresh, S. 2007. Biomechanics and biophysics of cancer cells. *Acta Mater.* 55:3989–4014.
6. Smith, J. F., T. P. Knowles, …, M. E. Welland. 2006. Characterization of the nanoscale properties of individual amyloid fibrils. *Proc. Natl. Acad. Sci. U S A.* 103:15806–15811.
7. Flurkey, K., J. Papaconstantinou, …, D. E. Harrison. 2001. Lifespan extension and delayed immune and collagen aging in mutant mice with defects in growth hormone production. *Proc. Natl. Acad. Sci. U S A.* 98:6736–6741.
8. Koester, K. J., H. D. Barth, and R. O. Ritchie. 2011. Effect of aging on the transverse toughness of human cortical bone: evaluation by R-curves. *J. Mech. Behav. Biomed. Mater.* 4:1504–1513.
9. Johnstone, I. L. 2000. Cuticle collagen genes: expression in *Caenorhabditis elegans*. *Trends Genet.* 16:21–27.
10. McMahon, L., J. M. Muriel, …, I. L. Johnstone. 2003. Two sets of interacting collagens form functionally distinct substructures within a *Caenorhabditis elegans* extracellular matrix. *Mol. Biol. Cell.* 14:1366–1378.
11. Ewald, C. Y., J. N. Landis, …, T. K. Blackwell. 2015. Dauer-independent insulin/IGF-1-signalling implicates collagen remodelling in longevity. *Nature.* 519:97–101.
12. Park, S., M. B. Goodman, and B. L. Pruitt. 2007. Analysis of nematode mechanics by piezoresistive displacement clamp. *Proc. Natl. Acad. Sci. U S A.* 104:17376–17381.
13. Elmi, M., V. M. Pawar, …, M. A. Srinivasan. 2017. Determining the biomechanics of touch sensation in *C. elegans*. *Sci. Rep.* 7:1–12.
14. Hochmuth, R. M. 2000. Micropipette aspiration of living cells. *J. Biomech.* 33:15–22.
15. Neuman, K. C., and S. M. Block. 2004. Optical trapping. *Rev. Sci. Instrum.* 75:2787–2809.
16. Essmann, C. L., M. Elmi, …, M. A. Srinivasan. 2017. In-vivo high resolution AFM topographic imaging of *Caenorhabditis elegans* reveals previously unreported surface structures of cuticle mutants. *Nanomedicine.* 13:183–189.
17. Tanase, M., N. Biais, and M. Sheetz. 2007. Magnetic tweezers in cell biology. *Methods Cell Biol.* 83:473–493.
18. Petzold, B. C., S. Park, …, B. L. Pruitt. 2013. MEMS-based force-clamp analysis of the role of body stiffness in *C. elegans* touch sensation. *Integr. Biol.* 5:853–864.
19. Gilpin, W., S. Uppaluri, and C. P. Brangwynne. 2015. Worms under pressure: bulk mechanical properties of *C. elegans* are independent of the cuticle. *Biophys. J.* 108:1887–1898.

20. Essmann, C. L., D. Martinez-Martinez, …, M. A. Srinivasan. 2020. Mechanical properties measured by atomic force microscopy define health biomarkers in ageing *C. elegans*. *Nat. Commun.* 11:1–16.

21. Wheeler, J. M., and J. H. Thomas. 2006. Identification of a novel gene family involved in osmotic stress response in *Caenorhabditis elegans*. *Genetics.* 174:1327–1336.

22. Reed, R. H., J. A. Chudek, …, G. M. Gadd. 1987. Osmotic significance of glycerol accumulation in exponentially growing yeasts. *Appl. Environ. Microbiol.* 53:2119–2123.

23. Cox, G. N., M. Kusch, and R. S. Edgar. 1981. Cuticle of *Caenorhabditis elegans*: its isolation and partial characterization. *J. Cell Biol.* 90:7–17.

24. Fordyce, P. M., C. A. Diaz-Botia, …, R. Gomez-Sjoberg. 2012. Systematic characterization of feature dimensions and closing pressures for microfluidic valves produced via photoresist reflow. *Lab Chip.* 12:4287–4295.

25. McDonald, J. C., and G. M. Whitesides. 2002. Poly (dimethylsiloxane) as a material for fabricating microfluidic devices. *Acc. Chem. Res.* 35:491–499.

26. Christensen, M., A. Estevez, …, K. Strange. 2002. A primary culture system for functional analysis of *C. elegans* neurons and muscle cells. *Neuron.* 33:503–514.

27. Herndon, L. A., P. J. Schmeissner, …, M. Driscoll. 2002. Stochastic and genetic factors influence tissue-specific decline in ageing *C. elegans*. *Nature.* 419:808–814.

28. Cox, G. N., C. Fields, …, D. Hirsh. 1989. Sequence comparisons of developmentally regulated collagen genes of *Caenorhabditis elegans*. *Gene.* 76:331–344.

29. von Mende, N., D. M. Bird, …, D. L. Riddle. 1988. Dpy-13: a nematode collagen gene that affects body shape. *Cell.* 55:567–576.

30. Dodd, W., L. Tang, …, K. P. Choe. 2018. A damage sensor associated with the cuticle coordinates three core environmental stress responses in *Caenorhabditis elegans*. *Genetics.* 208:1467–1482.

31. Thein, M. C., G. McCormack, …, A. P. Page. 2003. *Caenorhabditis elegans* exoskeleton collagen COL-19: an adult-specific marker for collagen modification and assembly, and the analysis of organismal morphology. *Dev. Dyn.* 226:523–539.

32. Kenyon, C., J. Chang, …, R. Tabtiang. 1993. A *C. elegans* mutant that lives twice as long as wild type. *Nature.* 366:461–464.

33. Murphy, C. T., S. A. McCarroll, …, C. Kenyon. 2003. Genes that act downstream of DAF-16 to influence the lifespan of *Caenorhabditis elegans*. *Nature.* 424:277–283.

34. Lee, S., C. T. Murphy, and C. Kenyon. 2009. Glucose shortens the life span of *C. elegans* by downregulating DAF-16/FOXO activity and aquaporin gene expression. *Cell Metab.* 10:379–391.

35. Finch, C. E., and G. Ruvkun. 2001. The genetics of aging. *Annu. Rev. Genomics Hum. Genet.* 2:435–462.

36. Tatar, M., A. Bartke, and A. Antebi. 2003. The endocrine regulation of aging by insulin-like signals. *Science.* 299:1346–1351.

37. Tanaka, H., F. A. Dinenno, …, D. R. Seals. 2000. Aging, habitual exercise, and dynamic arterial compliance. *Circulation.* 102:1270–1275.

38. Gates, P. E., and D. R. Seals. 2006. Decline in large elastic artery compliance with age: a therapeutic target for habitual exercise. *Br. J. Sports Med.* 40:897–899.

39. Zieman, S. J., V. Melenovsky, and D. A. Kass. 2005. Mechanisms, pathophysiology, and therapy of arterial stiffness. *Arterioscler. Thromb. Vasc. Biol.* 25:932–943.

40. Nakajima, M., M. R. Ahmad, …, T. Fukuda. 2009. Local stiffness measurements of *C. elegans* by buckling nanoprobes inside an environmental SEM. *In* 2009 IEEE/RSJ International Conference on Intelligent Robots and Systems, pp. 4695–4700.